

## Visualization of Peroxynitrite-Induced Changes of Labile $Zn^{2+}$ in the Endoplasmic Reticulum with Benzoresorufin-based Fluorescent Probes

Wei Lin, Daniela Buccella, and Stephen J. Lippard\*

### Table of Contents

<b>Figure S1</b>	$^1H$ NMR spectrum of ZBR1	2
<b>Figure S2</b>	$^{13}C\{^1H\}$ NMR spectrum of ZBR1	2
<b>Figure S3</b>	$^1H$ NMR spectrum of ZBR2	3
<b>Figure S4</b>	$^{13}C\{^1H\}$ NMR spectrum of ZBR2	3
<b>Figure S5</b>	$^1H$ NMR spectrum of ZBR3	4
<b>Figure S6</b>	$^{13}C\{^1H\}$ NMR spectrum of ZBR3	4
<b>Figure S7</b>	Molecular structure of ZBR3	5
<b>Table S1</b>	Crystal intensity, collection and refinement data	6
<b>Figure S8</b>	Absorption and emission spectra of ZBR2	7
<b>Figure S9</b>	Absorption and emission spectra of ZBR3	7
<b>Figure S10</b>	Plot of the normalized integrated emission intensity of ZBR2 with pH	8
<b>Figure S11</b>	Plot of the normalized integrated emission intensity of ZBR3 with pH	8
<b>Figure S12</b>	Integrated emission intensity of ZBR2 vs. $[Zn^{2+}]_{free}$ in aqueous buffer	9
<b>Figure S13</b>	Metal selectivity of ZBR2 in PIPES buffer solution	9
<b>Figure S14</b>	Metal selectivity of ZBR3 in PIPES buffer solution	10
<b>Figure S15</b>	Cytotoxicity of the ZBR sensors	10
<b>Figure S16</b>	Representative images of ZBR2 response to exogenous $Zn^{2+}$ in HeLa cells	11
<b>Figure S17</b>	Representative images of ZBR3 response to exogenous $Zn^{2+}$ in HeLa cells	11
<b>Figure S18</b>	Representative images of co-localization analysis of ZBR1 with organelle-specific dyes in HeLa cells	12
<b>Figure S19</b>	Representative images of co-localization analysis of ZBR1 with ER tracker in RAW 246.7 cells	13
<b>Figure S20</b>	Representative images of co-localization analysis of ZBR1 with ER tracker in NSCs	14
<b>Figure S21</b>	Representative images of co-localization analysis of ZBR2 with ER tracker in RAW 246.7 cells	15
<b>Figure S22</b>	Representative images of co-localization analysis of ZBR3 with ER tracker in RAW 246.7 cells	16
<b>Figure S23</b>	Extended view of co-localization analysis of ZBR1 with ER tracker and Mito tracker in HeLa cells	17
<b>Figure S24</b>	Effect of Sin-1 on the absorption response and fluorescence emission of ZBR1 and ZBR1- $Zn^{2+}$ complex	19

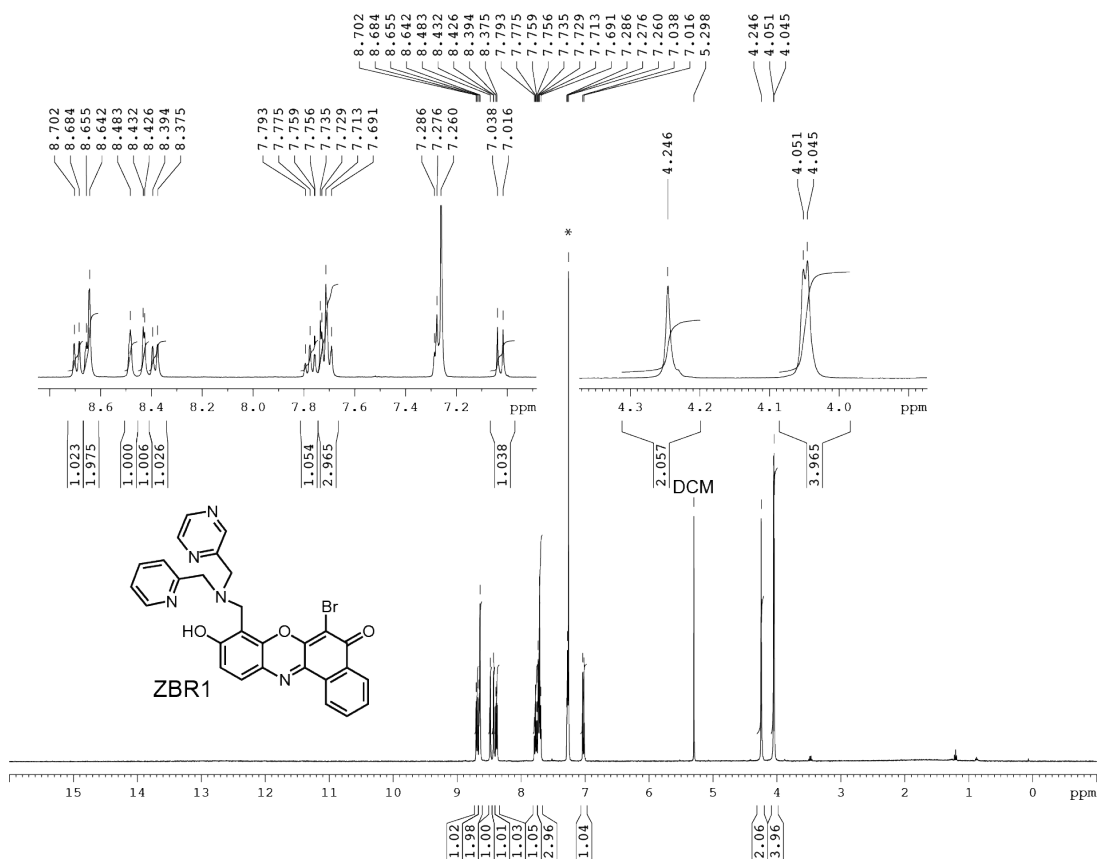


Figure S1.  $^1\text{H}$  NMR spectrum of ZBR1

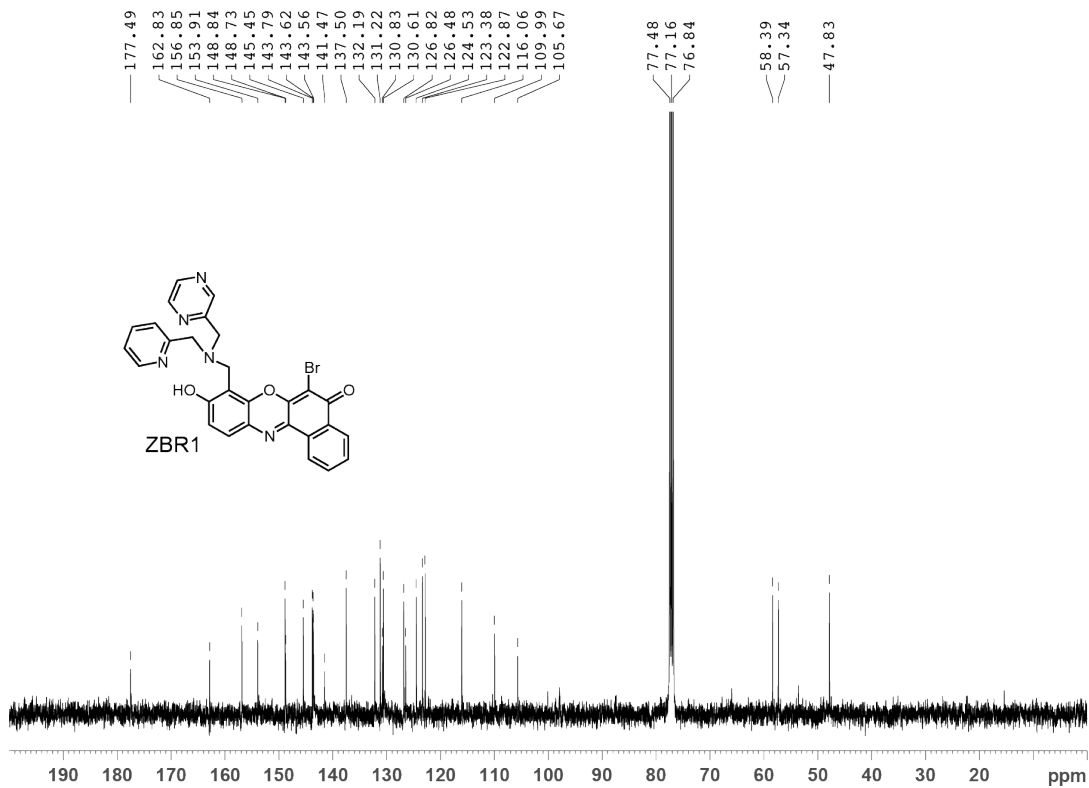
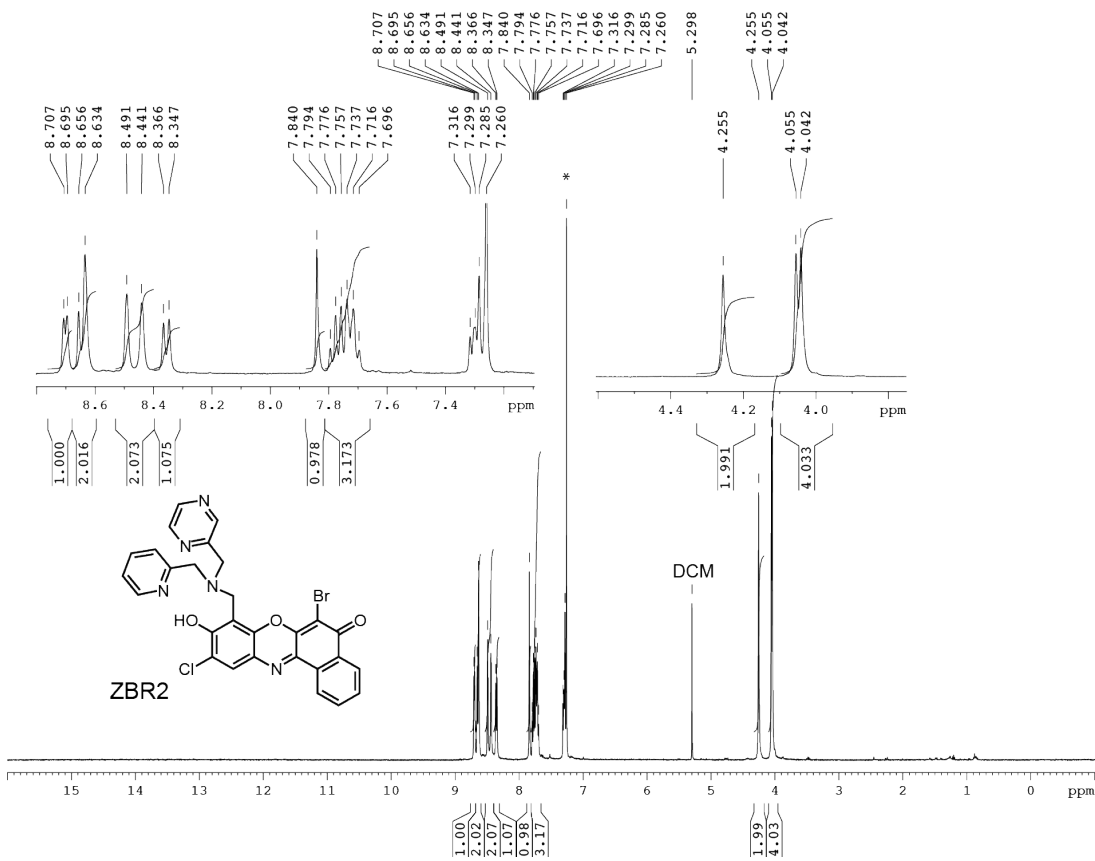
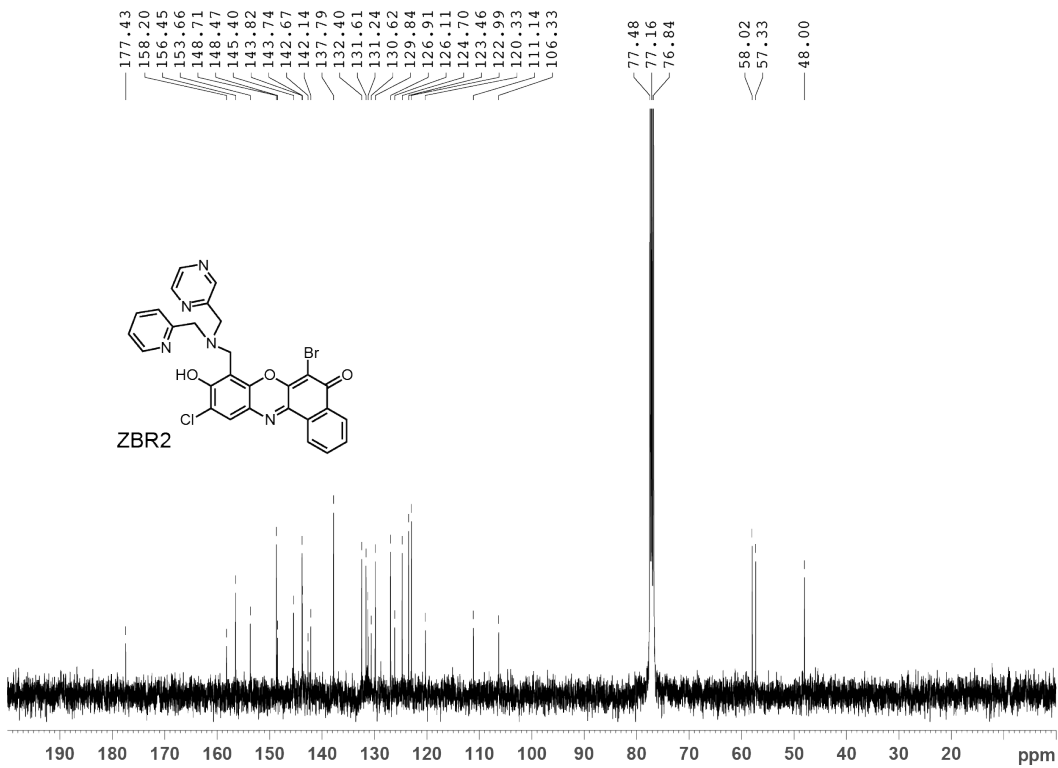


Figure S2.  $^{13}\text{C}\{^1\text{H}\}$  NMR spectrum of ZBR1



**Figure S3.  $^1\text{H}$  NMR spectrum of ZBR2**



**Figure S4.  $^{13}\text{C}\{^1\text{H}\}$  NMR spectrum of ZBR2**

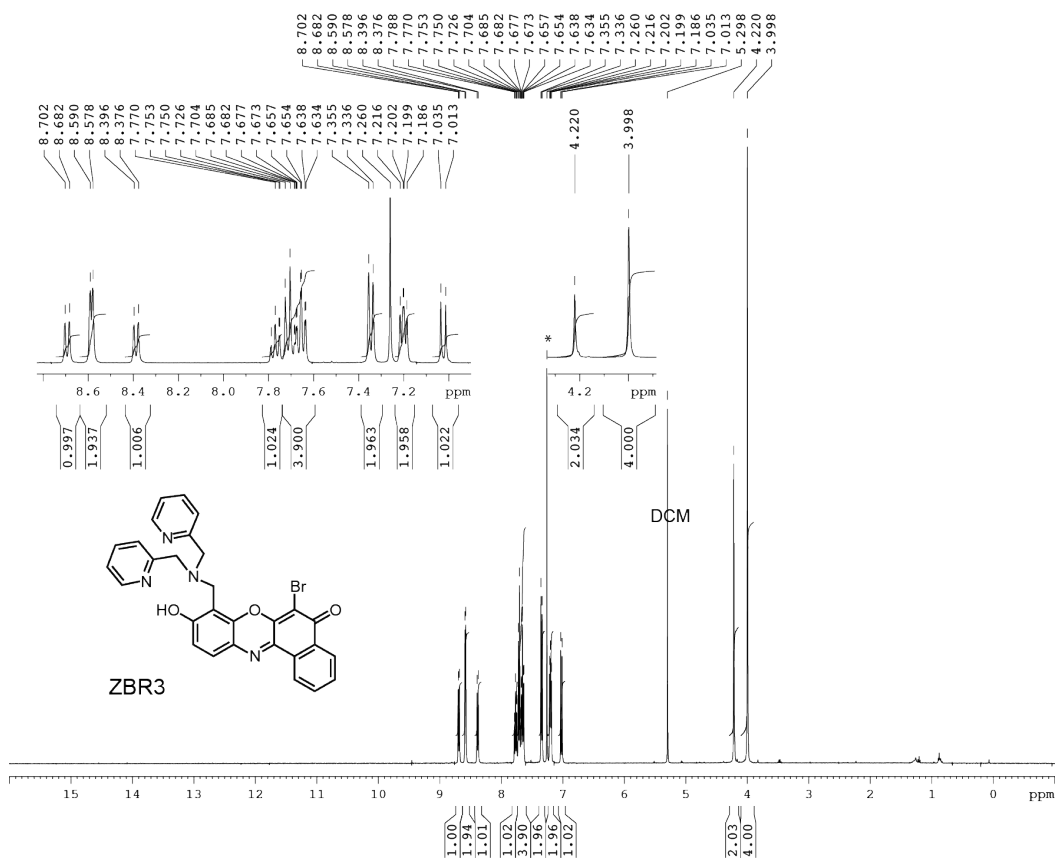


Figure S5. <sup>1</sup>H NMR spectrum of ZBR3

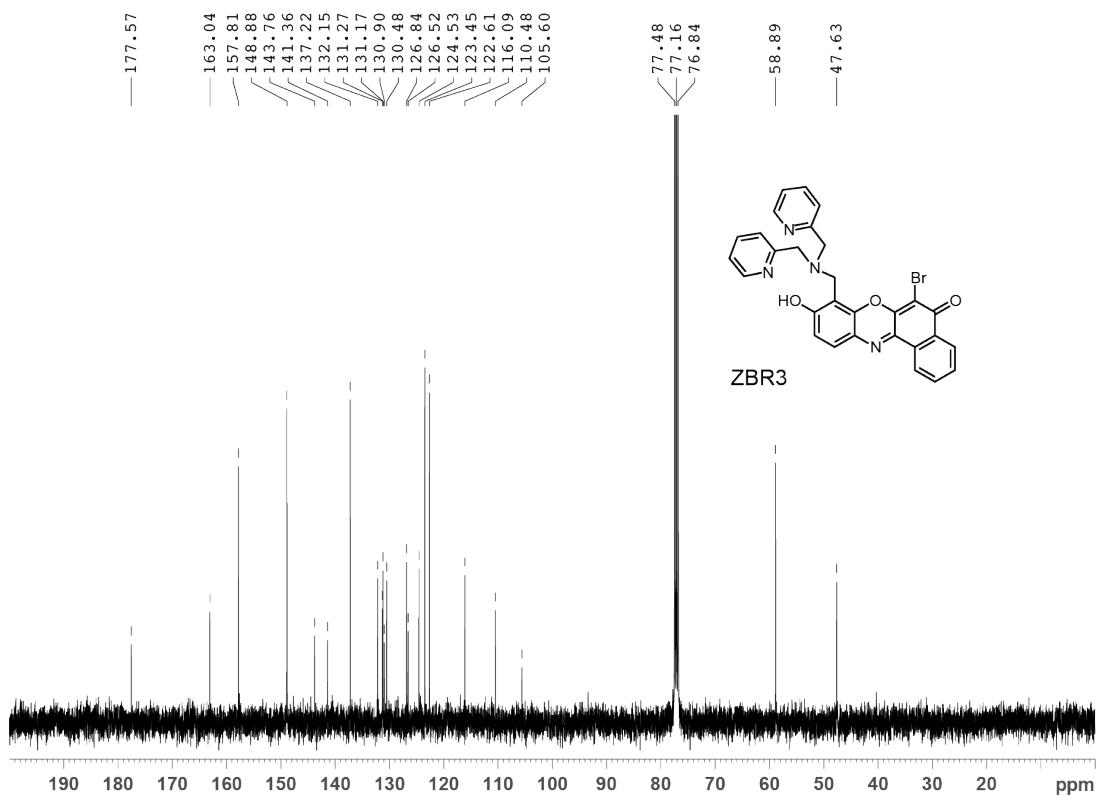
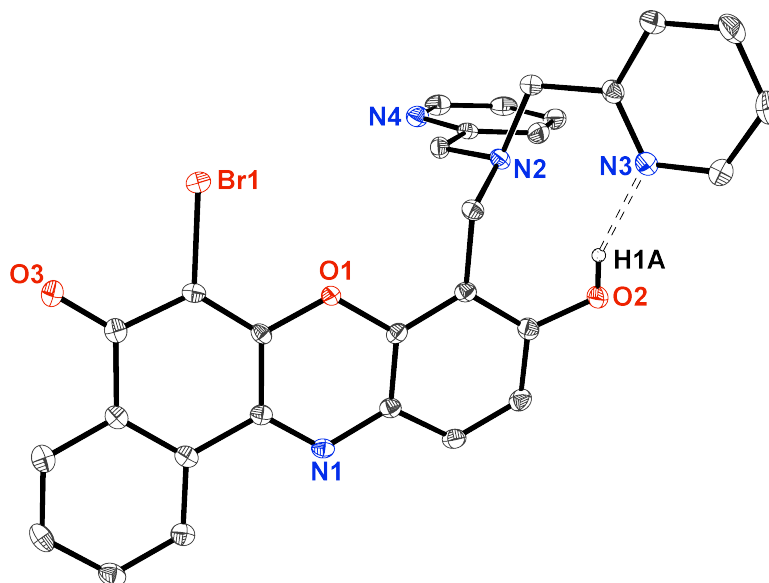


Figure S6. <sup>13</sup>C{<sup>1</sup>H} NMR spectrum of ZBR3



**Figure S7.** Molecular structure of ZBR3. ORTEP with 50% probability thermal ellipsoids.

**Table S1.** Crystal intensity, collection, and refinement data

ZBR3	
Crystal Lattice	Triclinic
Formula	C <sub>29</sub> H <sub>21</sub> BrN <sub>4</sub> O <sub>3</sub>
Formula weight	553.41
Space group	P $\bar{1}$
<i>a</i> /Å	9.1364(5)
<i>b</i> /Å	10.9864(6)
<i>c</i> /Å	12.3620(7)
$\alpha$ /°	78.8360(10)
$\beta$ /°	81.9300(10)
$\gamma$ /°	77.0540(10)
<i>V</i> /Å <sup>3</sup>	1180.30(11)
<i>Z</i>	2
Temperature (K)	100(2)
Radiation ( $\lambda$ , Å)	0.71073
$\rho$ (calcd.), g cm <sup>-3</sup>	1.557
$\mu$ (Mo K $\alpha$ ), mm <sup>-1</sup>	1.783
$\theta$ max, deg.	26.37
Completeness to $\theta$ (%)	99.9
No. of data	4842
No. of restraints	0
No. of parameters	335
R <sub>1</sub> [ <i>I</i> >2 $\sigma$ ( <i>I</i> )]	0.0256
wR <sub>2</sub> [ <i>I</i> >2 $\sigma$ ( <i>I</i> )]	0.0693
GOF	1.076

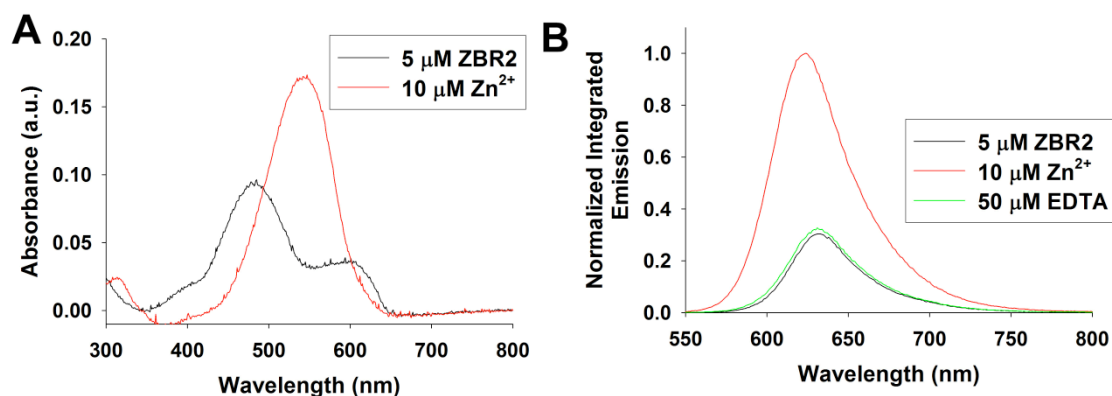


**Figure S8.** Absorption (A) and normalized fluorescence emission (B) spectra of ZBR2 in the absence and in the presence of excess Zn<sup>2+</sup>. Spectra were acquired on 5 μM solutions of ZBR2 in 100 mM KCl, 50 mM PIPES, pH 7.0 at 25 °C, after the addition of 10 μM ZnCl<sub>2</sub>, followed by 50 μM EDTA. Excitation was performed at 530 nm.

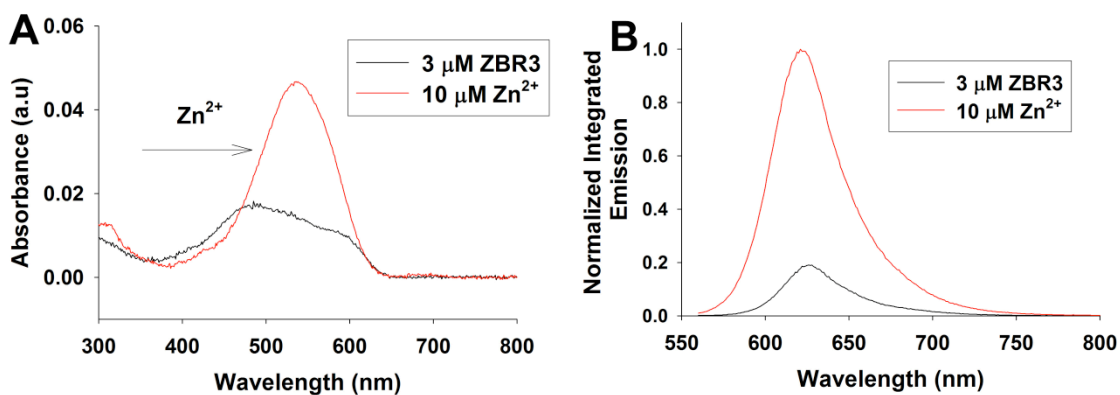


**Figure S9.** Absorption (A) and normalized fluorescence emission (B) spectra of ZBR3 in the absence and in the presence of excess Zn<sup>2+</sup>. Spectra were acquired on 3 μM solutions of ZBR3 in 100 mM KCl, 50 mM PIPES, pH 7.0 at 25 °C, after the addition 10 μM ZnCl<sub>2</sub>. Excitation was performed at 535 nm.

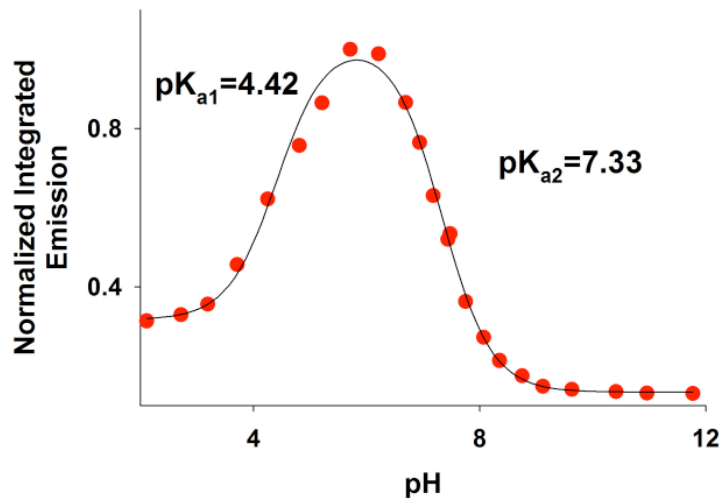


**Figure S10.** Plot of normalized integrated emission of ZBR2 vs. pH. The  $pK_a$  values were obtained from fitting the experimental data to a nonlinear model (continuous line).

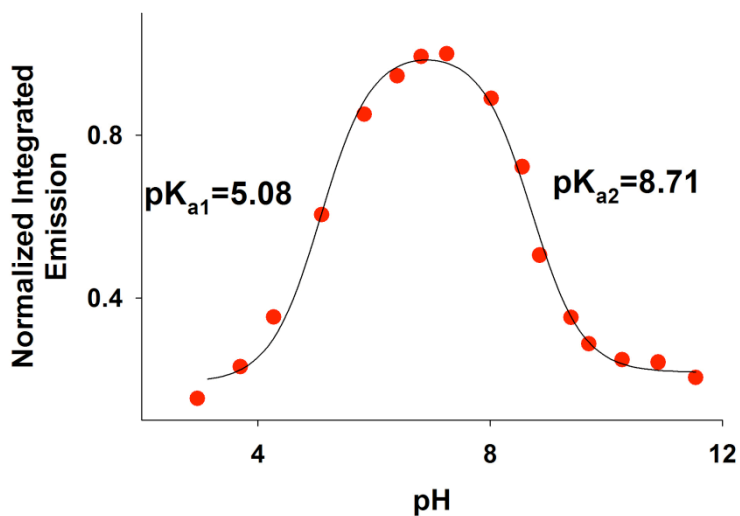


**Figure S11.** Plot of normalized integrated emission of ZBR3 vs. pH. The  $pK_a$  values were obtained from fitting the experimental data to a nonlinear model (continuous line).



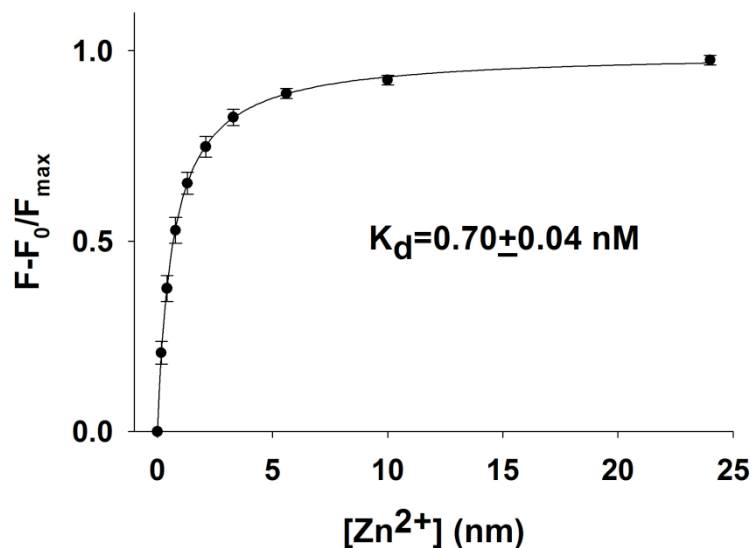


**Figure S12.** Integrated emission intensity of 1  $\mu\text{M}$  ZBR2 vs.  $[\text{Zn}^{2+}]_{\text{free}}$  in aqueous buffer at 25  $^{\circ}\text{C}$  (100 mM KCl, 50 mM PIPES, pH 7.0). Excitation was provided at 530 nm.

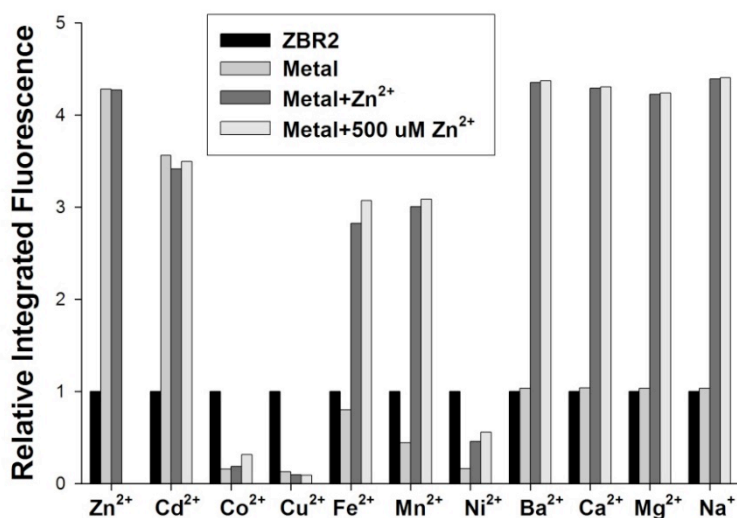


**Figure S13.** Metal selectivity of ZBR2 in PIPES buffer solution at pH 7.0. 5  $\mu\text{M}$  ZBR2 was mixed with 50  $\mu\text{M}$  of the metal ion of interest (gray) and then subsequently treated with 50  $\mu\text{M}$  (dark gray) or 500  $\mu\text{M}$  (light gray)  $\text{ZnCl}_2$ . Emission spectra was integrated from 550 nm to 800 nm. The integrated fluorescence after each addition was normalized to the fluorescence of the metal-free sensor.  $\lambda_{\text{ex}} = 530$  nm.

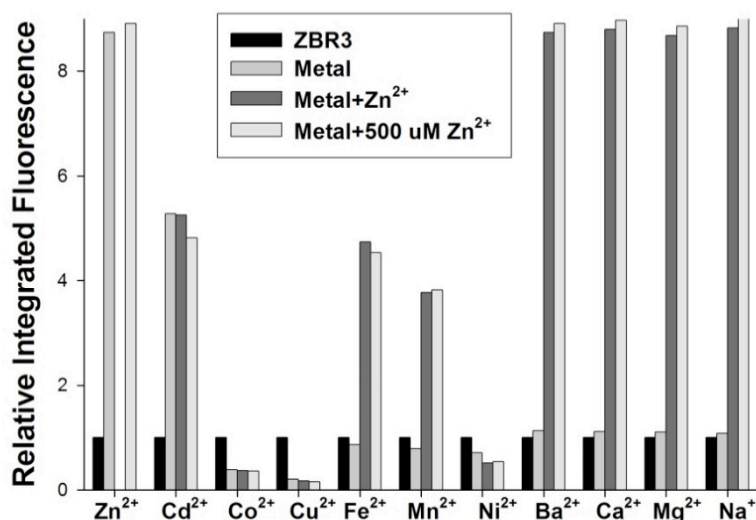


**Figure S14.** Metal selectivity of ZBR3 in PIPES buffer solution at pH 7.0. 5  $\mu\text{M}$  ZBR3 was mixed with 50  $\mu\text{M}$  of the metal ion of interest (gray) and then subsequently treated with 50  $\mu\text{M}$  (dark gray) or 500  $\mu\text{M}$  (light gray)  $\text{ZnCl}_2$ . Emission spectra were integrated from 550 nm to 800 nm. The integrated fluorescence after each addition was normalized to the fluorescence of the metal-free sensor.  $\lambda_{\text{ex}} = 535 \text{ nm}$ .

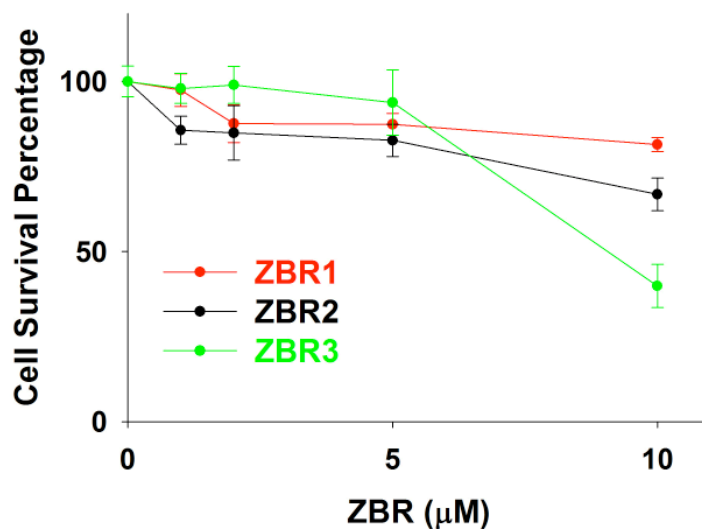


**Figure S15.** Cytotoxicity of the ZBR sensors applied to HeLa cells treated with different concentrations of ZBR1 (red), ZBR2 (black) and ZBR3 (green) for 24 h, measured by MTT assay. The data points represent the averages of three independent trials.

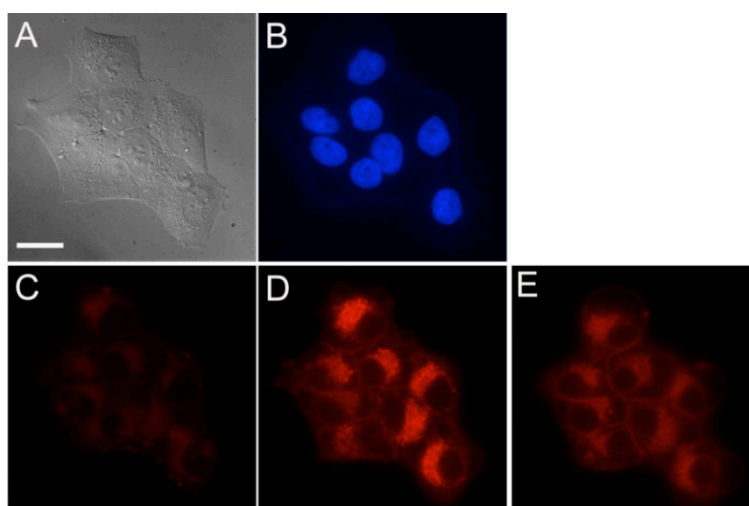


**Figure S16.** Representative images of ZBR2 response to exogenous  $\text{Zn}^{2+}$  in HeLa cells. Cells were incubated with 5  $\mu\text{M}$  ZBR2 and 5  $\mu\text{M}$  Hoechst 33258 at 37 °C for 30 min. A) Bright-field transmission image. B) Nuclear image stained by Hoechst 33258. C) Fluorescence image without addition of exogenous  $\text{Zn}^{2+}$ . D) Fluorescence image after addition of 25  $\mu\text{M}$   $\text{Zn}^{2+}$ /pyrithione (1:2). E) Fluorescence image 5 min after treatment with 50  $\mu\text{M}$  TPA. Scale bar = 25  $\mu\text{m}$ .

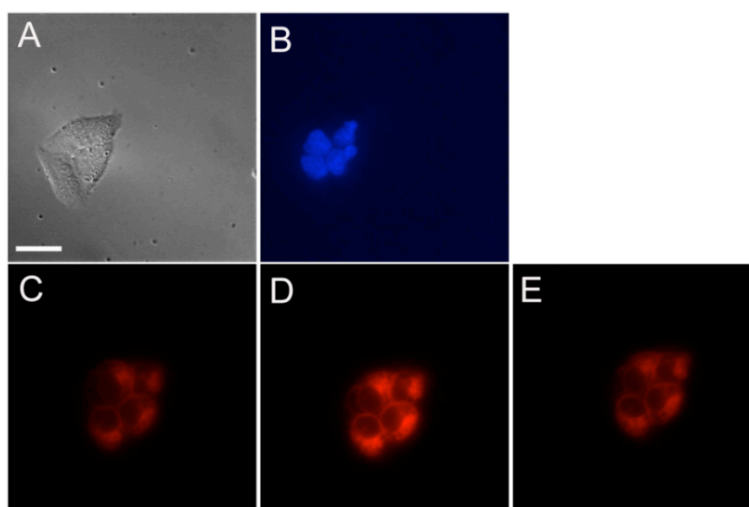


**Figure S17.** Representative images of ZBR3 response to exogenous  $\text{Zn}^{2+}$  in HeLa cells. Cells were incubated with 5  $\mu\text{M}$  ZBR2 and 5  $\mu\text{M}$  Hoechst 33258 at 37 °C for 30 min. A) Bright-field transmission image. B) Nuclear image stained by Hoechst 33258. C) Fluorescence image without addition of exogenous  $\text{Zn}^{2+}$ . D) Fluorescence image after addition of 25  $\mu\text{M}$   $\text{Zn}^{2+}$ /pyrithione (1:2). E) Fluorescence image 5 min after treatment with 50  $\mu\text{M}$  TPA. Scale bar = 25  $\mu\text{m}$ .

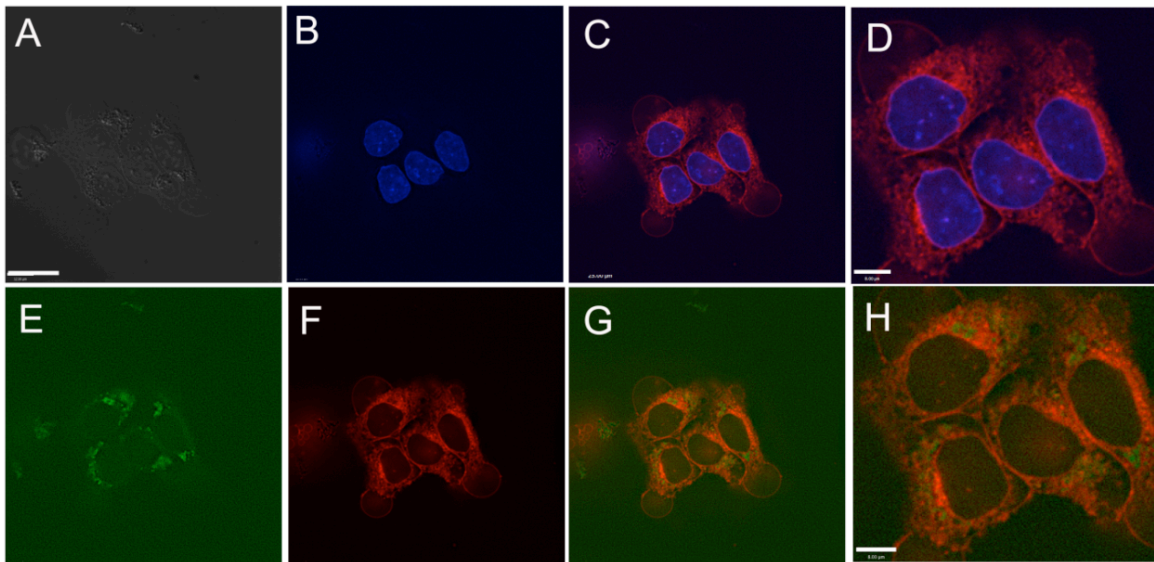


**Figure S18.** Representative images of co-localization analysis of ZBR1 with organelle-specific dyes in HeLa cells. Cells were incubated with 5  $\mu\text{M}$  ZBR1, 5  $\mu\text{M}$  Hoechst 33258 for 30 min. Golgi specific staining BacMam 2.0 was incubated at 10 PPC for 24 h to transduce HeLa cells. HeLa cells were then treated with 25  $\mu\text{M}$   $\text{Zn}^{2+}$ /pyrithione (1:2) on the microscope stage. A) Bright-field image. B) Nuclear image stained by Hoechst 33258. C) Overlay of ZBR1 and Hoechst 33258. D) Zoom-in of image C. E) BacMam 2.0 for Golgi staining. F) ZBR1. F) Overlay of ZBR1 and BacMam 2.0. H) Zoom-in of image G. Scale bar = 25  $\mu\text{m}$  or 8  $\mu\text{m}$  (for D and H).

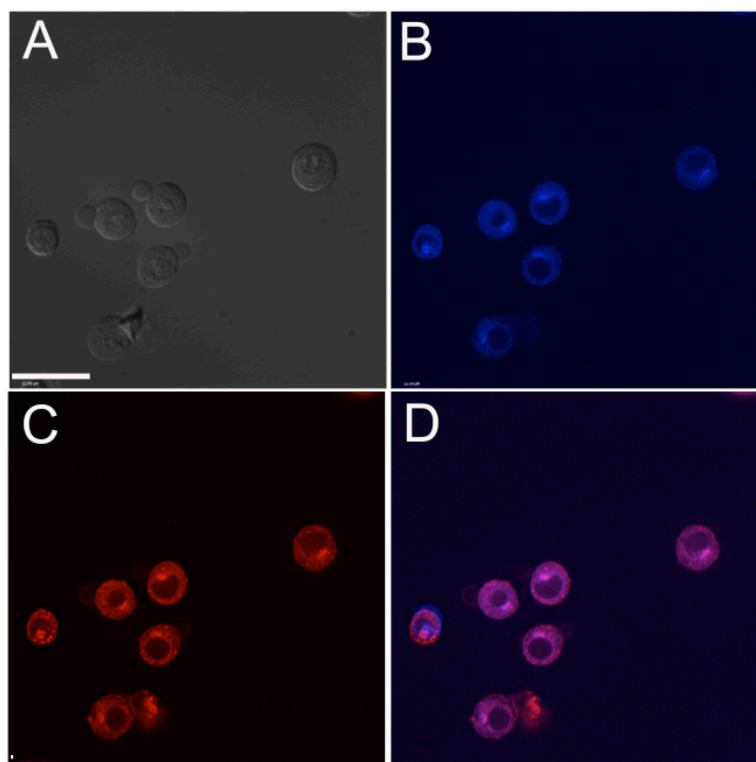


**Figure S19.** Representative images of co-localization analysis of ZBR1 with ER-Tracker in RAW 246.7 cells. Cells were incubated with 5  $\mu\text{M}$  ZBR1, 1  $\mu\text{M}$  ER-Tracker for 30 min. Cells were then treated with 25  $\mu\text{M}$   $\text{Zn}^{2+}$ /pyrithione (1:2) on the microscope stage. A) Bright-field image. B) Fluorescence image by ER-Tracker. C) Fluorescence image by ZBR1. D) Overlay of ZBR1 and ER-Tracker. Scale bar = 25  $\mu\text{m}$ .

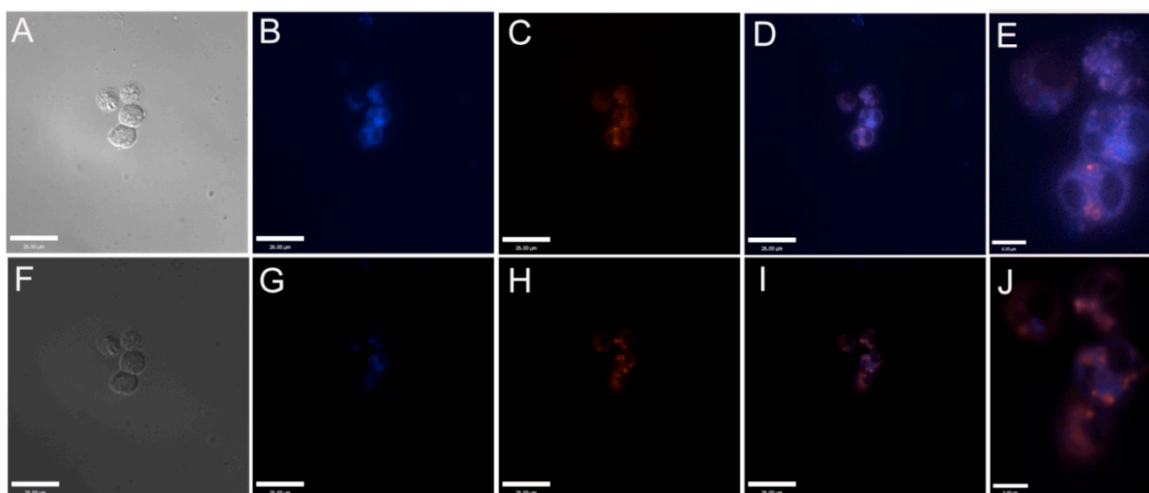


**Figure S20.** Representative images of co-localization analysis of ZBR1 with ER-Tracker in NSCs. Cells were incubated with 5  $\mu\text{M}$  ZBR1, 1  $\mu\text{M}$  ER-Tracker for 30 min. NSCs were then treated with 25  $\mu\text{M}$   $\text{Zn}^{2+}$ /pyrithione (1:2) on the microscope stage. A) Bright-field image. B) Fluorescence image by ER-Tracker. C) Fluorescence image by ZBR1. D) Overlay of ZBR1 and ER-Tracker. E) Zoom-in of image D. F) 2D-view of Bright-field image from integrated images. G) 2D-view of fluorescence image of ER-Tracker from integrated images. H) 2D-view of fluorescence image of ZBR1 from integrated images. I) Overlay of ZBR1 and ER-Tracker. J) Zoom-in of image I. Scale bar = 26  $\mu\text{m}$  or 6  $\mu\text{m}$  (for E and J).

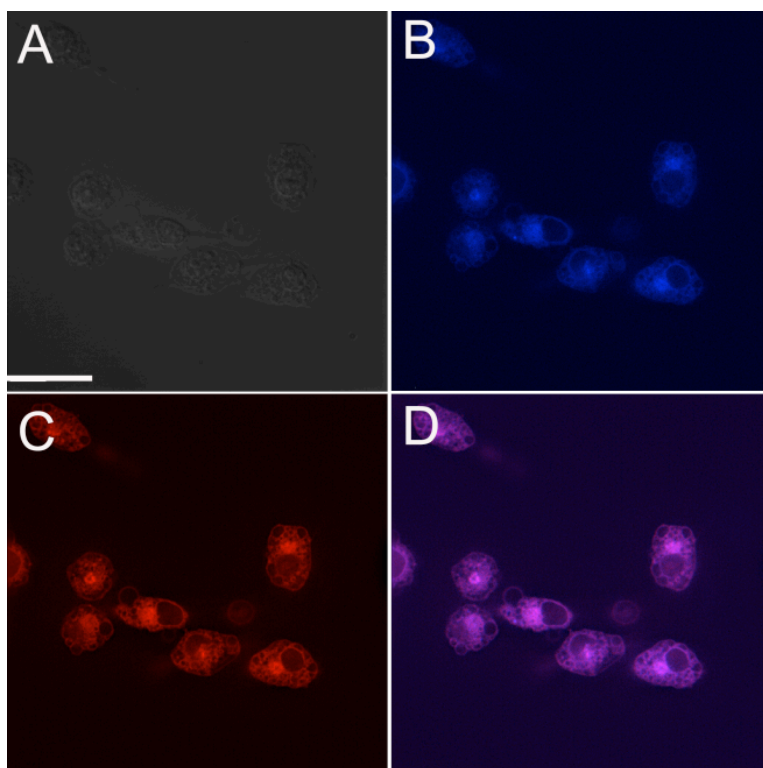


**Figure S21.** Representative images of co-localization analysis of ZBR2 with ER-Tracker in RAW 246.7 cells. Cells were incubated with 5  $\mu\text{M}$  ZBR2, 1  $\mu\text{M}$  ER-Tracker for 30 min. RAW 246.7 cells were then treated with 25  $\mu\text{M}$   $\text{Zn}^{2+}$ /pyrithione (1:2) on the microscope stage. A) Bright-field image. B) Fluorescence image of ER-Tracker. C) Fluorescence image of ZBR2. D) Overlay of ZBR2 and ER-Tracker. Scale bar = 25  $\mu\text{m}$ .

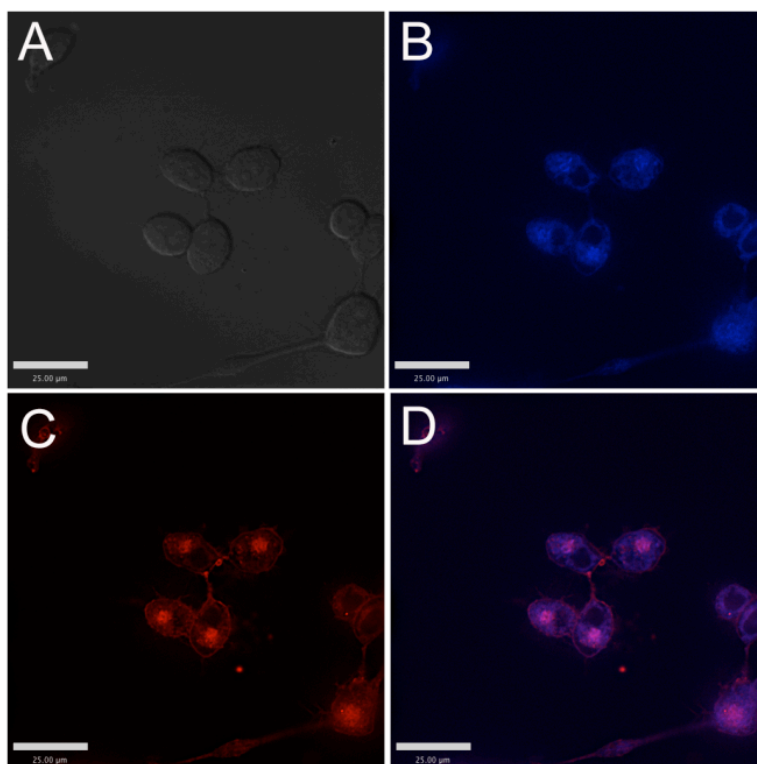


**Figure S22.** Representative images of co-localization analysis of ZBR3 with ER-Tracker in RAW 246.7 cells. Cells were incubated with 5  $\mu\text{M}$  ZBR3, 1  $\mu\text{M}$  ER-Tracker for 30 min. RAW 246.7 cells were then treated with 25  $\mu\text{M}$   $\text{Zn}^{2+}$ /pyrithione (1:2) on the microscope stage. A) Bright-field image. B) Fluorescence image of ER-Tracker. C) Fluorescence image of ZBR3. D) Overlay of ZBR3 and ER-Tracker. Scale bar = 25  $\mu\text{m}$



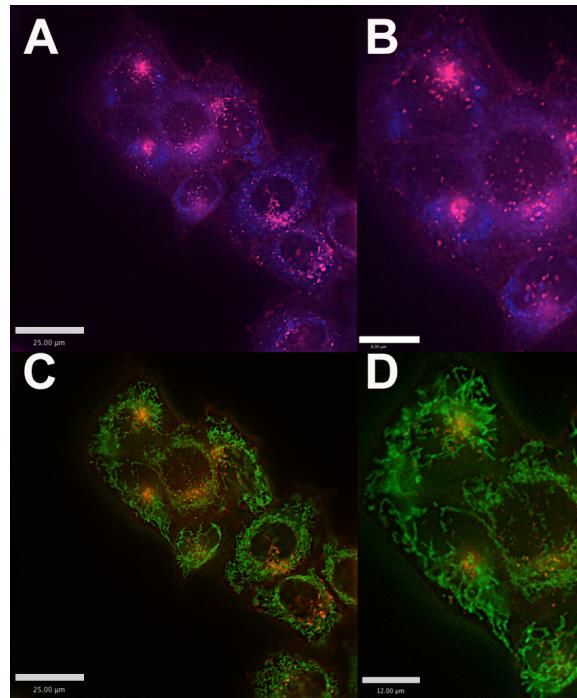


**Figure S23.** Colocalization analysis of ZBR1 with organelle-specific markers in HeLa cells incubated with 5  $\mu\text{M}$  ZBR1, 1  $\mu\text{M}$  ER tracker and 0.2  $\mu\text{M}$  MitoTracker Green for 30 min, and then treated with 25  $\mu\text{M}$   $\text{Zn}^{2+}$ /pyrithione (1:2) on the microscope stage. A) Overlay of ZBR1 and ER-Tracker. B) Zoom-in of panel A. C) Overlay of ZBR1 and MitoTracker Green. D) Zoom-in of panel C. Scale bar = 25  $\mu\text{m}$  (A and C), or 12  $\mu\text{m}$  (B D and D).

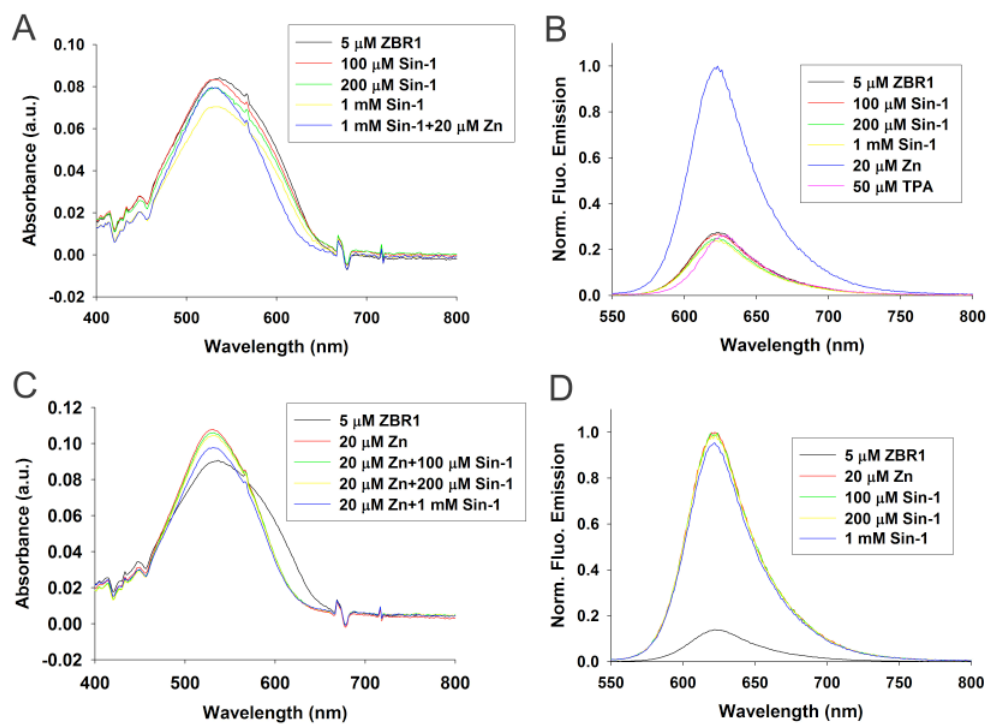


**Figure S24.** Effect of Sin-1 on the absorption and fluorescence emission of ZBR1 and ZBR1-Zn<sup>2+</sup> complex. Spectra were acquired in 100 mM KCl, 50 mM PIPES, pH 7.0 at 25 °C. A) Absorption spectra of 5 μM ZBR1 after the sequential addition of 100, 200 μM, 1 mM Sin-1 and 20 μM ZnCl<sub>2</sub>. B) Emission spectra of 5 μM ZBR1 after the sequential addition of 100, 200 μM, 1 mM Sin-1 and 20 μM ZnCl<sub>2</sub>. C) Absorption spectra of 5 μM ZBR1 after the addition of 20 μM ZnCl<sub>2</sub>, 100, 200 μM and 1 mM Sin-1. D) Emission spectra of 5 μM ZBR1 after the addition of 20 μM ZnCl<sub>2</sub>, 100, 200 μM and 1 mM Sin-1. Excitation wavelength was provided at 525 nm. Emission data were normalized to the response of the maximum fluorescence.